energies

MDPI

Article

Thermal Decomposition of Anhydrous Alkali Metal Dodecaborates $M_2B_{12}H_{12}$ (M = Li, Na, K)

Liqing He [1], Hai-Wen Li [2,3,*] and Etsuo Akiba [1,2,3]

Received: 16 July 2015 ; Accepted: 22 October 2015 ; Published: 4 November 2015
Academic Editor: Craig M. Jensen

1 Department of Mechanical Engineering, Faculty of Engineering, Kyushu University, Fukuoka 819-0395, Japan; he.liqing.401@s.kyushu-u.ac.jp (L.H.); e.akiba@mech.kyushu-u.ac.jp (E.A.)
2 International Research Center for Hydrogen Energy, Kyushu University, Fukuoka 819-0395, Japan
3 International Institute for Carbon-Neutral Energy Research (WPI-I2CNER), Kyushu University, Fukuoka 819-0395, Japan
* Correspondence: li.haiwen.305@m.kyushu-u.ac.jp; Tel.: +81-92-802-3226; Fax: +81-92-802-3235

Abstract: Metal dodecaborates $M_{2/n}B_{12}H_{12}$ are regarded as the dehydrogenation intermediates of metal borohydrides $M(BH_4)_n$ that are expected to be high density hydrogen storage materials. In this work, thermal decomposition processes of anhydrous alkali metal dodecaborates $M_2B_{12}H_{12}$ (M = Li, Na, K) synthesized by sintering of MBH_4 (M = Li, Na, K) and $B_{10}H_{14}$ have been systematically investigated in order to understand its role in the dehydrogenation of $M(BH_4)_n$. Thermal decomposition of $M_2B_{12}H_{12}$ indicates multistep pathways accompanying the formation of H-deficient monomers $M_2B_{12}H_{12-x}$ containing the icosahedral B_{12} skeletons and is followed by the formation of $(M_2B_{12}H_z)_n$ polymers. The decomposition behaviors are different with the *in situ* formed $M_2B_{12}H_{12}$ during the dehydrogenation of metal borohydrides.

Keywords: thermal decomposition; dodecaborate; borohydride; hydrogen storage; hydrogen

1. Introduction

Metal dodecaborates $M_{2/n}B_{12}H_{12}$ (n is the valence of M) have been widely regarded as a dehydrogenation intermediate of metal borohydrides $M(BH_4)_n$ with a high gravimetric hydrogen density of 10 mass% [1–16]. The formation of $M_{2/n}B_{12}H_{12}$, despite is still controversial, largely depends on the dehydrogenation temperature, hydrogen backpressure, particle size and sample pretreatment [11–21]. Due to the strong B-B bonds in an icosahedral boron cage B_{12}, the intermediate comprising of polyatomic anion $[B_{12}H_{12}]^{2-}$ has been widely regarded at the main obstacle for the rehydrogenation of $M(BH_4)_n$ [5,22–24]. Systematic investigation on the thermal decomposition of $M_{2/n}B_{12}H_{12}$ is therefore of great importance to understand their role in the dehydrogenation of $M(BH_4)_n$.

$M_{2/n}B_{12}H_{12}$ is generally synthesized using liquid phase reactions, followed by careful dehydration processes [25]. However, in some $M_{2/n}B_{12}H_{12}$ such as $MgB_{12}H_{12}$, the coordination water tends to form a hydrogen bond with the polyatomic anion $[B_{12}H_{12}]^{2-}$, resulting in the failure of dehydration [26]. To solve such problems, we have recently successfully developed a novel solvent-free synthesis process, *i.e.*, sintering of $M(BH_4)_n$ and $B_{10}H_{14}$ with stoichiometric molar ratio. Several anhydrous metal dodecaborates $M_{2/n}B_{12}H_{12}$ (M = Li, Na, K, Mg, Ca, LiNa), so far, have been successfully synthesized via the newly developed method [21,27,28].

In this work, we carefully investigate the thermal decomposition behaviors of anhydrous alkali metal dodecaborates $M_2B_{12}H_{12}$ (M = Li, Na, K) that are synthesized using the reported method [27]. Furthermore, the roles of $M_2B_{12}H_{12}$ (M = Li, Na, K) in the dehydrogenation of corresponding

borohydrides MBH_4 are discussed, based on the comparison of the decomposition pathways of $M_2B_{12}H_{12}$ and those *in situ* formed during the decomposition of MBH_4.

2. Results and Discussion

2.1. Decomposition of Anhydrous $Li_2B_{12}H_{12}$

Figure 1 shows the thermogravimetry (TG) and mass spectrometry (MS) measurement results of anhydrous $Li_2B_{12}H_{12}$. Only hydrogen is detected in MS, indicating that the weight loss upon heating results from the dehydrogenation. The weight loss starts at approximately 200 °C and the dehydrogenation amount reaches 5.1 mass% (approximately 66% of the theoretical hydrogen content in $Li_2B_{12}H_{12}$) when heated up to 700 °C. The decomposition proceeds with multistep reactions, as shown in TG and MS results.

In order to investigate the decomposition process of anhydrous $Li_2B_{12}H_{12}$, the sample was heated to respective temperatures and subsequently cooled down to room temperature. The changes examined by X-ray diffraction (XRD), Raman and nuclear magnetic resonance (NMR) are shown in Figures 2 and 3 respectively. When the temperature is increased to 250 °C, no obvious changes of XRD patterns, Raman spectra and the main resonance at −15.3 ppm for $Li_2B_{12}H_{12}$ are observed, whereas the resonance at −41.3 ppm originated from residual $LiBH_4$ decreases significantly and those at 11.2 ppm and −36.0 ppm for the unknown side product disappears (Table 1). This indicates that anhydrous $Li_2B_{12}H_{12}$ is stable up to 250 °C and the weight loss of 0.3 mass% up to 250 °C is originated from decomposition of the residual $LiBH_4$ and side product. When the temperature is increased to 300 °C, intensities for the diffraction peaks (2θ = 15.8° and 18.4°) and Raman spectra (between 500–1000 cm^{-1} and around 2500 cm^{-1}) attributed to $Li_2B_{12}H_{12}$ decrease. This indicates that anhydrous $Li_2B_{12}H_{12}$ starts to decompose above 250 °C, similar to the reported temperature [16]. The resonance at −29.8 ppm originated from $Li_2B_{10}H_{10}$ and that at −17.5 ppm for the unknown side product become significantly weaker when heated up to 300 °C and completely disappear when heated up to 500 °C. When the temperature is increased to 600 °C, diffraction peaks and Raman spectra attributed to $Li_2B_{12}H_{12}$ nearly disappear, and the main resonances at −15.3 ppm for ^{11}B and at 1.4 ppm for ^{1}H originated from $Li_2B_{12}H_{12}$ decrease significantly without any change in the chemical shift. This indicates that a major part of B–H bond in the icosahedral polyatomic anion $[B_{12}H_{12}]^{2-}$ has been broken to release hydrogen [21]. The dehydrogenation amount reaches 3.7 mass% including the contribution from the residual $LiBH_4$ and side products, suggesting that the decomposition product is probably H-deficient $Li_2B_{12}H_{12-x}$ ($x < 5.3$) that remains the icosahedral B_{12} skeletons [16,21]. No signals in the solution-state ^{11}B NMR were detected, implying that the formed $Li_2B_{12}H_{12-x}$ is DMSO insoluble. When the temperature is further increased to 700 °C, the dehydrogenation amount reaches 5.1 mass%, the major resonance of $Li_2B_{12}H_{12}$ at −15.3 ppm in ^{11}B MAS NMR shifts to −11.9 ppm, and that at 1.4 ppm in ^{1}H MAS NMR changes to several weak resonance peaks from −10 ppm to 10 ppm. This suggests that $Li_2B_{12}H_{12-x}$ continuously releases hydrogen accompanied by the polymerization of the icosahedral B_{12} skeletons and the formation of $(Li_2B_{12}H_z)_n$ polymers [15,21,29], insoluble in water and DMSO.

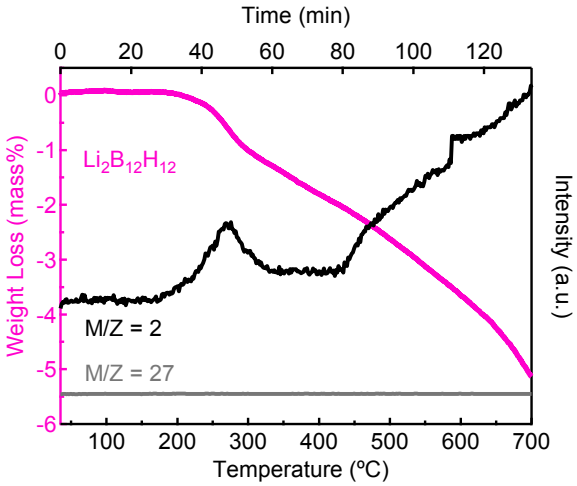

Figure 1. Thermogravimetry (TG) curve and mass spectrometry (MS) signals of anhydrous $Li_2B_{12}H_{12}$ (mass numbers 2 and 27 represent H_2 and B_2H_6).

Table 1. Relative amount of the B-H species in synthesized $Li_2B_{12}H_{12}$ when heated up to respective temperatures (⩽500 °C), estimated from the peak fitting of ^{11}B MAS NMR spectra shown in Figure 3.

Temperature, °C	$[B_{12}H_{12}]^{2-}$, %	$[B_{11}H_{11}]^{2-}$, %	$[B_{10}H_{10}]^{2-}$, %	$[BH_4]^-$, %	Unknown, %
200	60.93	9.03	18.76	5.14	6.14
225	65.82	9.50	12.16	3.76	8.76
250	70.17	10.00	17.21	2.62	0
300	71.62	11.70	16.20	0.48	0
400	86.52	0	13.48	0	0
500	100	0	0	0	0

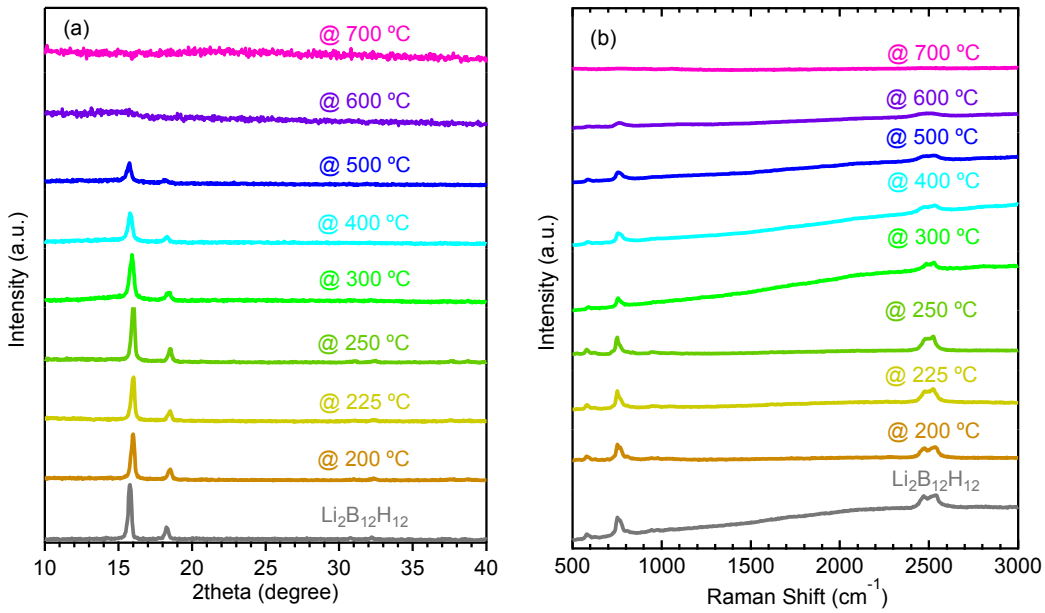

Figure 2. *Ex-situ* (**a**) X-ray diffraction (XRD) patterns and (**b**) Raman spectra of anhydrous $Li_2B_{12}H_{12}$ and heated up to respective temperatures.

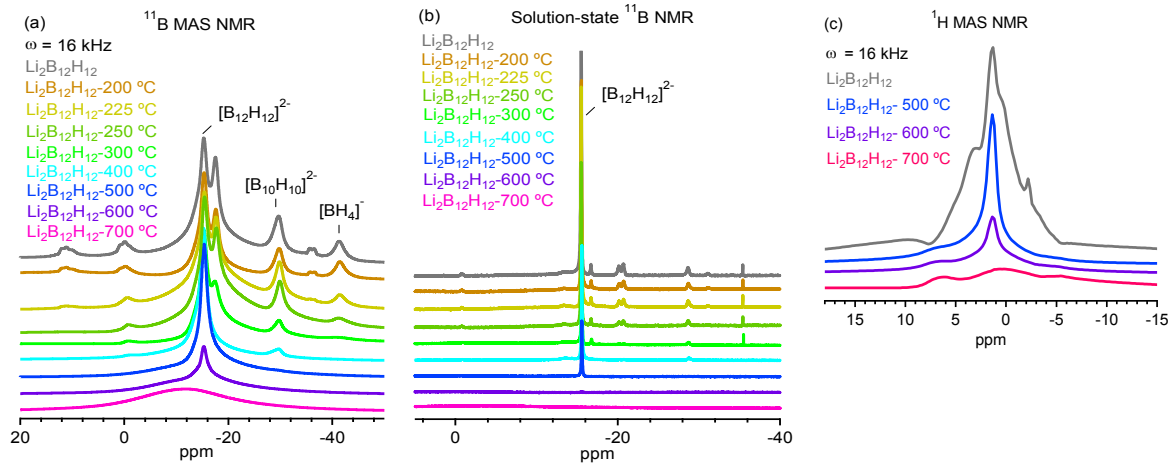

Figure 3. *Ex-situ* ^{11}B and ^{1}H NMR spectra of anhydrous $Li_2B_{12}H_{12}$ and heated up to respective temperatures: (**a**) solid-state ^{11}B MAS NMR spectra; (**b**) solution-state ^{11}B NMR spectra measured in DMSO-d_6 and (**c**) solid-state ^{1}H MAS NMR spectra. Resonance assignments of ^{11}B spectra: −15.6 ppm $[B_{12}H_{12}]^{2-}$, −35.6 ppm $[BH_4]^-$, −0.9 & −28.8 ppm $[B_{10}H_{10}]^{2-}$, −16.8 ppm $[B_{11}H_{11}]^{2-}$, −20.3 (−20.8) ppm $[B_9H_9]^{2-}$ [30]. Resonance assignments of ^{1}H spectra: 1.2 ppm $[B_{12}H_{12}]^{2-}$ [10,16].

The thermal decomposition pathway of anhydrous $Li_2B_{12}H_{12}$ up to 700 °C is, therefore, summarized based on the abovementioned experimental results:

$$\text{Step 1}: \ Li_2B_{12}H_{12} \rightarrow Li_2B_{12}H_{12-x} + x/2H_2 \quad (1)$$

$$\text{Step 2}: \ nLi_2B_{12}H_{12-x} \rightarrow (Li_2B_{12}H_z)_n + z'H_2 \quad (2)$$

The decomposition pathway is similar to those of anhydrous $MgB_{12}H_{12}$ and $CaB_{12}H_{12}$ [21]. It is worth noting that the thermal decomposition behaviors of anhydrous $Li_2B_{12}H_{12}$ are different from that *in situ* formed during the dehydrogenation of $LiBH_4$, like those of anhydrous $MgB_{12}H_{12}$ and $CaB_{12}H_{12}$ [21]. Anhydrous $Li_2B_{12}H_{12}$ shows a lower initial decomposition temperature and a wider decomposition temperature range of 250 ~>700 °C than those *in situ* formed during dehydrogenation of $LiBH_4$. The formation of $Li_2B_{12}H_{12}$ during the dehydrogenation of $LiBH_4$ generally experiences complicated condensation process with sluggish kinetics [11], attributing to the higher initial decomposition temperature than that of anhydrous $Li_2B_{12}H_{12}$. On the other hand, the high activity of the *in situ* formed $Li_2B_{12}H_{12}$ together with the concurrent formation of LiH facilitate the decomposition of $Li_2B_{12}H_{12}$ [8], resulting in the lower temperature of complete decomposition than that of anhydrous $Li_2B_{12}H_{12}$.

2.2. Decomposition of Anhydrous $Na_2B_{12}H_{12}$

Figure 4 shows the TG and MS measurement results of anhydrous $Na_2B_{12}H_{12}$. Only hydrogen is detected in MS, indicating that the weight loss is originated from the dehydrogenation. The weight loss starts at approximately 580 °C and the dehydrogenation amount reaches 1.9 mass%, which is approximately 29% of the theoretical hydrogen capacity in $Na_2B_{12}H_{12}$. The value is comparable to the reported one (~1.5 mass% at 697 °C) [31].

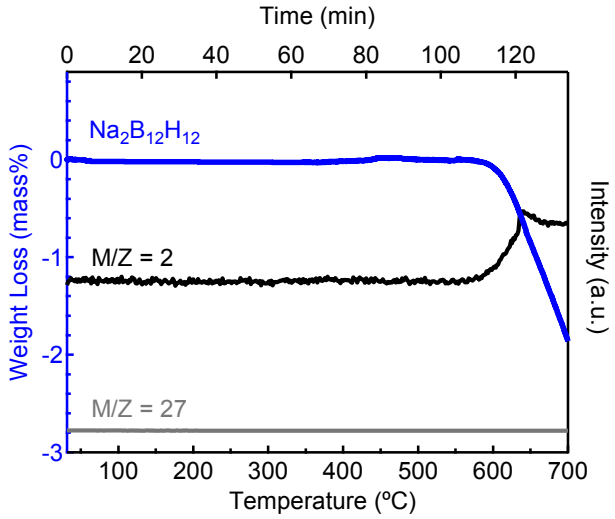

Figure 4. TG curve and MS signals of anhydrous $Na_2B_{12}H_{12}$ (mass numbers 2 and 27 represent H_2 and B_2H_6).

The changes of anhydrous $Na_2B_{12}H_{12}$ heated to respective temperatures and subsequently cooled down to room temperature examined by XRD, Raman and ^{11}B NMR are shown in Figures 5 and 6 respectively. When the temperature is increased to 500 °C, no obvious changes of diffraction peaks, Raman spectra and the major resonance at −15.7 ppm for $Na_2B_{12}H_{12}$ are observed, whereas the resonances originated from $NaBH_4$ and $Na_2B_{10}H_{10}$ nearly disappear. This suggests that the small amount of side product $Na_2B_{10}H_{10}$ and the residual $NaBH_4$ (<8 mass%) start to decompose below 500 °C without detected weight loss. When the temperature is increased to 600 °C, diffraction peaks and Raman spectra attributed to $Na_2B_{12}H_{12}$ becomes weak, indicating that $Na_2B_{12}H_{12}$ starts to decompose at 600 °C. When the temperature is further increased to 700 °C, diffraction peaks and Raman spectra from $Na_2B_{12}H_{12}$ are hardly observed, the main resonance at −15.7 ppm significantly weakens and a broad resonance between −12.4 ppm and −14.8 ppm appears. This suggests that the major dehydrogenation of $Na_2B_{12}H_{12}$ to H-deficient $Na_2B_{12}H_{12-x}$ and the polymerization of $Na_2B_{12}H_{12-x}$ to water and DMSO insoluble $(Na_2B_{12}H_z)_n$ polymers start to take place at 700 °C [15,21,29].

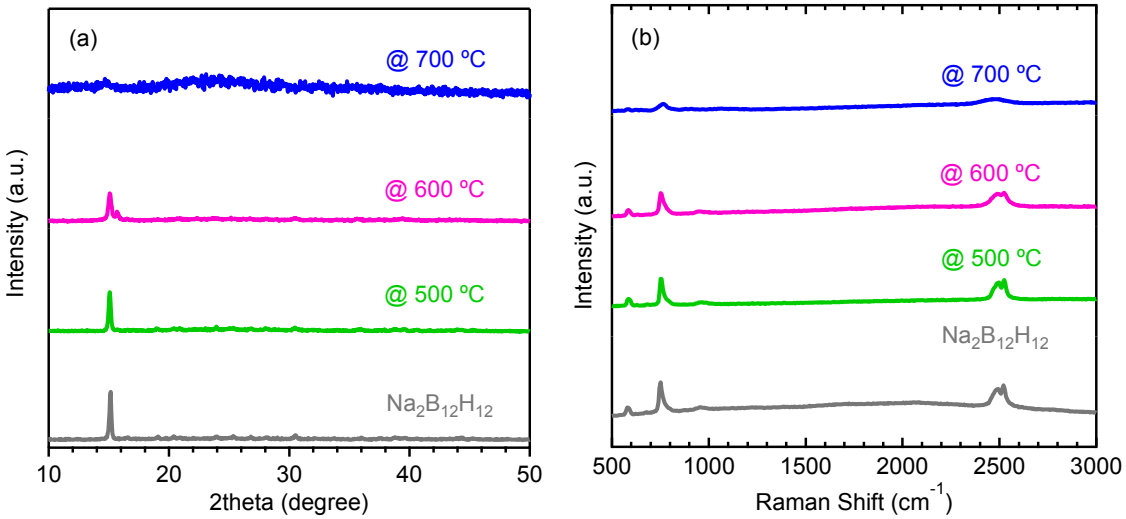

Figure 5. *Ex-situ* (**a**) XRD patterns and (**b**) Raman spectra of anhydrous $Na_2B_{12}H_{12}$ as synthesized and heated up to respective temperatures.

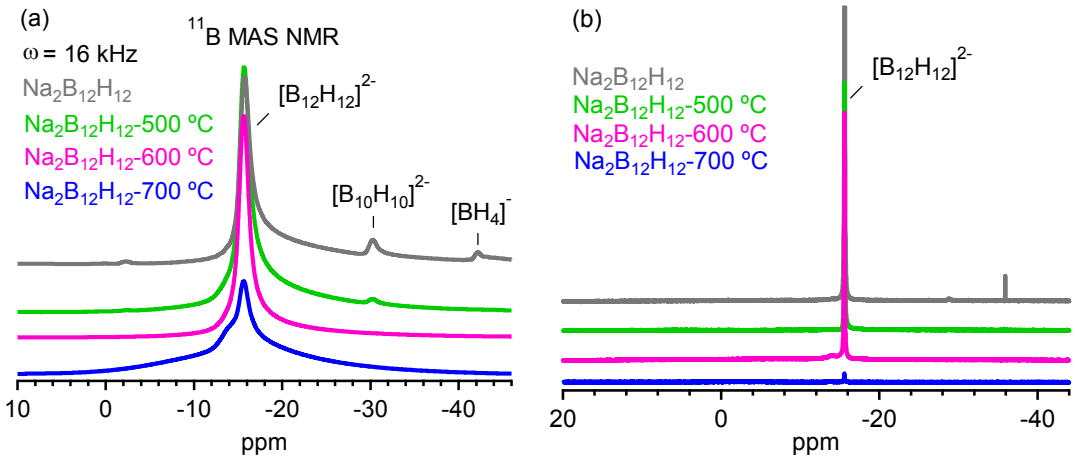

Figure 6. *Ex-situ* ^{11}B NMR spectra of anhydrous $Na_2B_{12}H_{12}$ as synthesized and heated up to respective temperatures: (**a**) solid-state ^{11}B MAS NMR spectra and (**b**) solution-state ^{11}B NMR spectra measured in DMSO-d_6. Resonance assignments: −15.6 ppm $[B_{12}H_{12}]^{2-}$, −35.9 ppm $[BH_4]^-$, −28.8 ppm $[B_{10}H_{10}]^{2-}$ [32].

2.3. Decomposition of Anhydrous $K_2B_{12}H_{12}$

Figure 7 shows the TG and MS results of anhydrous $K_2B_{12}H_{12}$. Only hydrogen is detected in MS, indicating that the weight loss upon heating results from the dehydrogenation. The weight loss starts at approximately 480 °C and the dehydrogenation amount reaches 4.4 mass% (approximately 80% of theoretical hydrogen capacity in $K_2B_{12}H_{12}$) when heated up to 700 °C. The dehydrogenation proceeds with multistep reactions, as shown in TG and MS results.

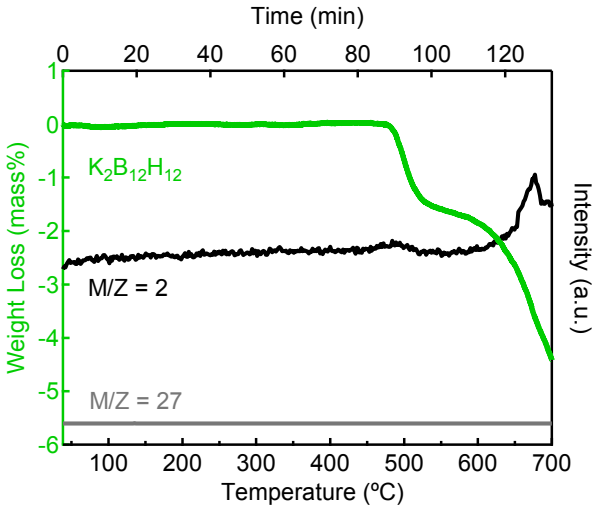

Figure 7. TG curve and MS signals of anhydrous $K_2B_{12}H_{12}$ (mass numbers 2 and 27 represent H_2 and B_2H_6).

The changes of anhydrous $K_2B_{12}H_{12}$ heated up to respective temperatures and subsequently cooled down to room temperature examined by XRD, Raman and ^{11}B NMR are shown in Figures 8 and 9 respectively. When the temperature is increased to 475 °C, no obvious changes of diffraction peaks, Raman spectra and the major resonance at −15.4 ppm attributed to $K_2B_{12}H_{12}$ are seen. The resonance originated from residual KBH_4 (−38.2 ppm in solid-state and −35.6 ppm in solution-state ^{11}B NMR) disappears when the temperature is increased to 550 °C, whereas no obvious changes of diffraction peaks, Raman spectra and the major resonance attributed to

$K_2B_{12}H_{12}$ are observed. This suggests that the weight loss bellow 550 °C is responsible for the dehydrogenation of residual KBH_4. When the temperature is increased to 625 °C, diffraction peaks, Raman spectra and the main resonance attributed to $K_2B_{12}H_{12}$ become weak slightly, indicating the partial decomposition of $K_2B_{12}H_{12}$ at 625 °C. It is worth noting that the initial thermal decomposition temperature increases with the order of $Li_2B_{12}H_{12}$ < $Na_2B_{12}H_{12}$ < $K_2B_{12}H_{12}$, which shows the same trend to the dehydrogenation temperature of corresponding metal borohydrides [33].

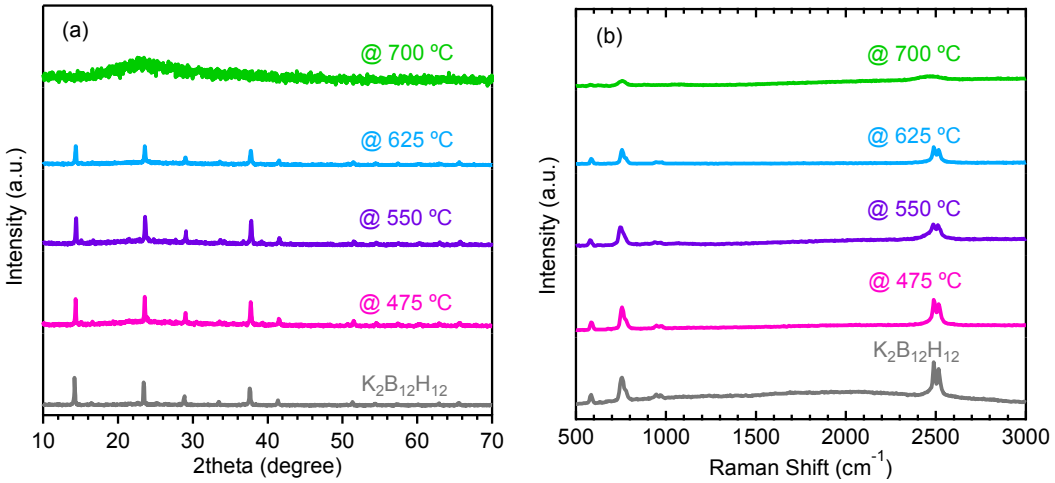

Figure 8. *Ex-situ* (**a**) XRD patterns and (**b**) Raman spectra of anhydrous $K_2B_{12}H_{12}$ as synthesized and heated up to respective temperatures.

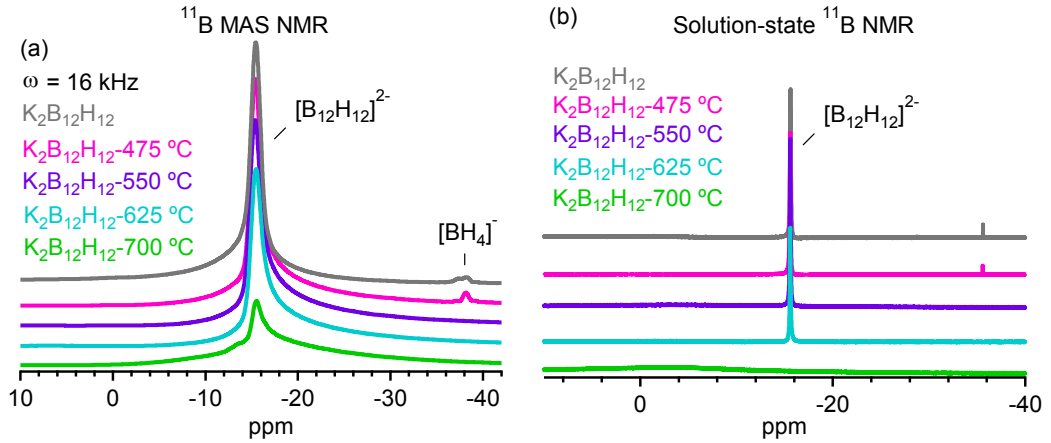

Figure 9. *Ex-situ* ^{11}B NMR spectra of anhydrous $K_2B_{12}H_{12}$ as synthesized and heated up to respective temperatures: (**a**) solid-state ^{11}B MAS NMR spectra and (**b**) solution-state ^{11}B NMR spectra measured in DMSO-d_6. Resonance assignments: –15.6 ppm $[B_{12}H_{12}]^{2-}$, –35.6 ppm $[BH_4]^-$ [32].

When the temperature is increased to 700 °C, the diffraction peaks and Raman spectra from $K_2B_{12}H_{12}$ are hardly observed, the main resonance at −15.4 ppm in ^{11}B MAS NMR decreases significantly without any change in the chemical shift and a broad resonance between −12.2 ppm and −14.2 ppm appears. It suggests that the major dehydrogenation of $K_2B_{12}H_{12}$ to $K_2B_{12}H_{12-x}$ and the polymerization of $K_2B_{12}H_{12-x}$ to $(K_2B_{12}H_z)_n$ polymers start to happen at 700 °C [21], similar to those of $Na_2B_{12}H_{12}$. Like $(Li_2B_{12}H_z)_n$ and $(Na_2B_{12}H_z)_n$ polymers, the produced $(K_2B_{12}H_z)_n$ polymers are also insoluble in water and DMSO. The decomposition behavior of anhydrous $K_2B_{12}H_{12}$ is different from that formed as a dehydrogenation intermediate of KBH_4 predicted by theoretical calculation [34], suggesting that the coexisting KH may facilitate the decomposition of $K_2B_{12}H_{12}$.

In summary, the thermal decomposition of anhydrous alkali metal dodecaborates $M_2B_{12}H_{12}$ (M = Li, Na, K) proceeds in two steps: (1) dehydrogenate to produce H-deficient $M_2B_{12}H_{12-x}$ containing the icosahedral B_{12} skeletons and (2) polymerization of $M_2B_{12}H_{12-x}$ to form $(M_2B_{12}H_z)_n$. Such behaviors are similar to those of anhydrous $MgB_{12}H_{12}$ and $CaB_{12}H_{12}$ [21], but fairly differ from those *in situ* formed during the dehydrogenation of $M(BH_4)_n$. These findings suggest that further investigations on the correlation between thermal decomposition behaviors of possible dehydrogenation intermediates and of the corresponding metal borohydrides are of great importance for the clarification of the dehydrogenation mechanism.

3. Experimental Section

Anhydrous $Li_2B_{12}H_{12}$, $Na_2B_{12}H_{12}$ and $K_2B_{12}H_{12}$ were synthesized by sintering of $B_{10}H_{14}$ with $LiBH_4$, $NaBH_4$ and KBH_4 (Sigma-Aldrich, Ichikawa, Japan), at 200–450 °C for 15–20 h [27]. All the synthesized anhydrous $Li_2B_{12}H_{12}$, $Na_2B_{12}H_{12}$ and $K_2B_{12}H_{12}$ were stored in glove box filled with purified Ar gas.

Powder XRD patterns were recorded by a Rigaku Ultima IV X-ray diffractometer with Cu-Kα radiation (Rigaku, Tokyo, Japan), and the accelerating voltage/tube current were set as 40 kV/40 mA. The sample powders were placed on a zero diffraction plate sealed by Scotch tape to prevent air exposure during the measurement. Raman spectra were obtained from a RAMAN-11 VIS-SS (Nanophoton, Osaka, Japan) using a green laser with 532 nm wavelength. Thermal decomposition was analyzed by TG (Rigaku), with a heating rate of 5 °C/min under a 200 mL/min flow of helium gas. The gas released during the TG measurement was analyzed by a quadrupole mass spectrometer coupled with TG. Solid-state MAS NMR spectra were recorded by a Bruker Ascend-600 spectrometer (Bruker, Yokohama, Japan), at room temperature. NMR sample preparations were always operated in a glove box filled with purified Ar gas and sample spinning was conducted using dry N_2 gas. ^{11}B MAS NMR spectra were obtained at excitation pulses of 6.5 μs (π/2 pulse) and with strong ^1H decoupling pulses. ^{11}B NMR chemical shifts were referenced to BF_3OEt_2 (δ = 0.00 ppm). ^1H MAS NMR spectra were obtained at excitation pulses of 6.5 μs (π/2 pulse) and the chemical shifts were referred to deuterated water (δ = 4.75 ppm). Solution-state ^{11}B NMR experiments were carried out using the same apparatus of Bruker Ascend-600 (Bruker), dimethyl sulfoxide (DMSO-d_6) was used as solvent and saturated $B(OH)_3$ aqueous solution at 19.4 ppm was used as external standard sample.

4. Conclusions

Systematic investigations of thermal decomposition indicate that anhydrous alkali metal dodecaborates $M_2B_{12}H_{12}$ (M = Li, Na, K) firstly dehydrogenate to produce the H-deficient $M_2B_{12}H_{12-x}$ containing the icosahedral B_{12} skeletons, followed by the polymerization of $M_2B_{12}H_{12-x}$ to form $(M_2B_{12}H_z)_n$ polymers, similar to those of anhydrous $MgB_{12}H_{12}$ and $CaB_{12}H_{12}$ [21]. No amorphous B was detected in all $M_2B_{12}H_{12}$ samples upon heating up to 700 °C, suggesting that higher temperature is needed for the complete decomposition of $(M_2B_{12}H_z)_n$. The initial thermal decomposition temperature increases with the order of $Li_2B_{12}H_{12}$ < $Na_2B_{12}H_{12}$ < $K_2B_{12}H_{12}$, which shows the same trend to the dehydrogenation temperature of corresponding borohydrides. The thermal decomposition behaviors of anhydrous $M_2B_{12}H_{12}$ are fairly different with those *in situ* formed during the dehydrogenation of corresponding metal borohydrides. Further investigations on the correlation between thermal decomposition of possible dehydrogenation intermediates and of the corresponding metal borohydrides are expected in order to clarify the exact dehydrogenation mechanism of metal borohydrides.

Acknowledgments: We would like to sincerely thank Miho Yamauchi and Motonori Watanabe in I2CNER for their great help on ^{11}B MAS NMR measurement. This study was partially supported by JSPS KAKENHI Grant No. 25709067 and the International Institute for Carbon Neutral Energy Research (WPI-I2CNER), sponsored by the Japanese Ministry of Education, Culture, Sports, Science and Technology.

Author Contributions: All of the authors contributed to this work. Liqing He and Hai-Wen Li designed and carried out the experiments. Liqing He, Hai-Wen Li and Etsuo Akiba analyzed the experimental results and wrote the manuscript.

Conflicts of Interest: The authors declare no conflict of interest.

References

1. Li, H.-W.; Yan, Y.; Orimo, S.-I.; Züttel, A.; Jensen, C.M. Recent progress in metal borohydrides for hydrogen storage. *Energies* **2011**, *4*, 185–214. [CrossRef]
2. Rude, L.H.; Nielsen, T.K.; Ravnsbaek, D.B.; Bösenberg, U.; Ley, M.B.; Richter, B.; Arnbjerg, L.M.; Dornheim, M.; Filinchuk, Y.; Besenbacher, F.; *et al*. Tailoring properties of borohydrides for hydrogen storage: A review. *Phys. Status Solidi A* **2011**, *208*, 1754–1773. [CrossRef]
3. Orimo, S.-I.; Nakamori, Y.; Ohba, N.; Miwa, K.; Aoki, M.; Towata, S.-I.; Zuttel, A. Experimental studies on intermediate compound of $LiBH_4$. *Appl. Phys. Lett.* **2006**, *89*. [CrossRef]
4. Ohba, N.; Miwa, K.; Aoki, M.; Noritake, T.; Towata, S.-I.; Nakamori, Y.; Orimo, S.-I.; Züttel, A. First-principles study on the stability of intermediate compounds of $LiBH_4$. *Phys. Rev. B* **2006**, *74*. [CrossRef]
5. Li, H.-W.; Kikuchi, K.; Nakamori, Y.; Ohba, N.; Miwa, K.; Towata, S.; Orimo, S. Dehydriding and rehydriding processes of well-crystallized $Mg(BH_4)_2$ accompanying with formation of intermediate compounds. *Acta Mater.* **2008**, *56*, 1342–1347. [CrossRef]
6. Hwang, S.-J.; Bowman, R.C.; Reiter, J.W.; Rijssenbeek, J.; Soloveichik, G.L.; Zhao, J.-C.; Kabbour, H.; Ahn, C.C. NMR confirmation for formation of $[B_{12}H_{12}]^{2-}$ complexes during hydrogen desorption from metal borohydrides. *J. Phys. Chem. C* **2008**, *112*, 3164–3169. [CrossRef]
7. Her, J.-H.; Yousufuddin, M.; Zhou, W.; Jalisatgi, S.S.; Kulleck, J.G.; Zan, J.A.; Hwang, S.-J.; Bowman, R.C., Jr.; Udovic, T.J. Crystal structure of $Li_2B_{12}H_{12}$: A possible intermediate species in the decomposition of $LiBH_4$. *Inorg. Chem.* **2008**, *47*, 9757–9759. [CrossRef] [PubMed]
8. Ozolins, V.; Majzoub, E.; Wolverton, C. First-Principles Prediction of Thermodynamically reversible hydrogen storage reactions in the Li-Mg-Ca-B-H system. *J. Am. Chem. Soc.* **2009**, *131*, 230–237. [CrossRef] [PubMed]
9. Li, H.-W.; Miwa, K.; Ohba, N.; Fujita, T.; Sato, T.; Yan, Y.; Towata, S.; Chen, M.; Orimo, S. Formation of an intermediate compound with a $B_{12}H_{12}$ cluster: Experimental and theoretical studies on magnesium borohydride $Mg(BH_4)_2$. *Nanotechnology* **2009**, *20*. [CrossRef] [PubMed]
10. Stavila, V.; Her, J.-H.; Zhou, W.; Hwang, S.-J.; Kim, C.; Ottley, L.A.M.; Udovic, T.J. Probing the structure, stability and hydrogen storage properties of calcium dodecahydro-*closo*-dodecaborate. *J. Solid State Chem.* **2010**, *183*, 1133–1140. [CrossRef]
11. Yan, Y.; Li, H.-W.; Maekawa, H.; Aoki, M.; Noritake, T.; Matsumoto, M.; Miwa, K.; Towata, S.-I.; Orimo, S.-I. Formation Process of $[B_{12}H_{12}]^{2-}$ from $[BH_4]^-$ during the Dehydrogenation Reaction of $Mg(BH_4)_2$. *Mater. Trans.* **2011**, *52*, 1443–1446. [CrossRef]
12. Bonatto Minella, C.; Garroni, S.; Olid, D.; Teixidor, F.; Pistidda, C.; Lindemann, I.; Gutfleisch, O.; Baró, M.D.; Bormann, R.; Klassen, T.; Dornheim, M. Experimental evidence of $Ca[B_{12}H_{12}]$ formation during decomposition of a $Ca(BH_4)_2$ + MgH_2 based reactive hydride composite. *J. Phys. Chem. C* **2011**, *115*, 18010–18014. [CrossRef]
13. Garroni, S.; Milanese, C.; Pottmaier, D.; Mulas, G.; Nolis, P.; Girella, A.; Caputo, R.; Olid, D.; Teixdor, F.; Baricco, M. Experimental evidence of $Na_2[B_{12}H_{12}]$ and Na formation in the desorption pathway of the $2NaBH_4$ + MgH_2 system. *J. Phys. Chem.C* **2011**, *115*, 16664–16671. [CrossRef]
14. Yan, Y.; Li, H.-W.; Maekawa, H.; Miwa, K.; Towata, S.; Orimo, S. Formation of intermediate compound $Li_2B_{12}H_{12}$ during the dehydrogenation process of the $LiBH_4$-MgH_2 system. *J. Phys. Chem. C* **2011**, *115*, 19419–19423. [CrossRef]
15. Yan, Y.; Remhof, A.; Hwang, S.-J.; Li, H.-W.; Mauron, P.; Orimo, S.-I.; Züttel, A. Pressure and temperature dependence of the decomposition pathway of $LiBH_4$. *Phys. Chem. Chem. Phys.* **2012**, *14*, 6514–6519. [CrossRef] [PubMed]
16. Pitt, M.P.; Paskevicius, M.; Brown, D.H.; Sheppard, D.A.; Buckley, C.E. Thermal Stability of $Li_2B_{12}H_{12}$ and Its Role in the Decomposition of $LiBH_4$. *J. Am. Chem. Soc.* **2013**, *135*, 6930–6941. [CrossRef] [PubMed]

17. Yan, Y.; Remhof, A.; Rentsch, D.; Züttel, A. The role of $MgB_{12}H_{12}$ in the hydrogen desorption process of $Mg(BH_4)_2$. *Chem. Commun.* **2015**, *51*, 700–702. [CrossRef] [PubMed]
18. Xia, G.; Meng, Q.; Guo, Z.; Gu, Q.; Liu, H.; Liu, Z.; Yu, X. Nanoconfinement significantly improves the thermodynamics and kinetics of co-infiltrated $2LiBH_4$-$LiAlH_4$ composites: Stable reversibility of hydrogen absorption/resorption. *Acta Mater.* **2013**, *61*, 6882–6893. [CrossRef]
19. Borgschulte, A.; Callini, E.; Probst, B.; Jain, A.; Kato, S.; Friedrichs, O.; Remhof, A.; Bielmann, M.; Ramirez-Cuesta, A.; Züttel, A. Impurity gas analysis of the decomposition of complex hydrides. *J. Phys. Chem. C* **2011**, *115*, 17220–17226. [CrossRef]
20. Stadie, N.P.; Callini, E.; Richter, B.; Jensen, T.R.; Borgschulte, A.; Züttel, A. Supercritical N_2 Processing as a Route to the Clean Dehydrogenation of Porous $Mg(BH_4)_2$. *J. Am. Chem. Soc.* **2014**, *136*, 8181–8184. [CrossRef] [PubMed]
21. He, L.; Li, H.-W.; Tumanov, N.; Filinchuk, Y.; Akiba, E. Facile synthesis of anhydrous alkaline earth metal dodecaborates $MB_{12}H_{12}$ (M = Mg, Ca) from $M(BH_4)_2$. *Dalton Trans.* **2015**, *44*, 15882–15887. [CrossRef] [PubMed]
22. Kim, Y.; Hwang, S.-J.; Shim, J.-H.; Lee, Y.-S.; Han, H.N.; Cho, Y.W. Investigation of the Dehydrogenation Reaction Pathway of $Ca(BH_4)_2$ and Reversibility of Intermediate Phases. *J. Phys. Chem. C* **2012**, *116*, 4330–4334. [CrossRef]
23. Li, H.-W.; Akiba, E.; Orimo, S.-I. Comparative study on the reversibility of pure metal borohydrides. *J. Alloy. Compd.* **2013**, *580*, S292–S295. [CrossRef]
24. Minella, C.B.; Pistidda, C.; Garroni, S.; Nolis, P.; Baró, M.D.; Gutfleisch, O.; Klassen, T.; Bormann, R.; Dornheim, M. $Ca(BH_4)_2$ + MgH_2: Desorption reaction and role of Mg on its reversibility. *J. Phys. Chem. C* **2013**, *117*, 3846–3852. [CrossRef]
25. Sivaev, I.B.; Bregadze, V.I.; Sjöberg, S. Chemistry of *closo*-Dodecaborate Anion $[B_{12}H_{12}]^{2-}$: A Review. *Collect. Czechoslov. Chem. Commun.* **2002**, *67*, 679–727. [CrossRef]
26. Chen, X.; Liu, Y.-H.; Alexander, A.-M.; Gallucci, J.C.; Hwang, S.-J.; Lingam, H.K.; Huang, Z.; Wang, C.; Li, H.; Zhao, Q.; *et al.* Desolvation and dehydrogenation of solvated magnesium salts of dodecahydrododecaborate: Relationship between structure and thermal decomposition. *Chem. A Eur. J.* **2014**, *20*, 7325–7333. [CrossRef] [PubMed]
27. He, L.; Li, H.-W.; Hwang, S.-J.; Akiba, E. Facile Solvent-Free Synthesis of Anhydrous Alkali Metal Dodecaborate $M_2B_{12}H_{12}$ (M= Li, Na, K). *J. Phys. Chem. C* **2014**, *118*, 6084–6089. [CrossRef]
28. He, L.; Li, H.-W.; Nakajima, H.; Tumanov, N.; Filinchuk, Y.; Hwang, S.-J.; Sharma, M.; Hagemann, H.; Akiba, E. Synthesis of a bimetallic dodecaborate $LiNaB_{12}H_{12}$ with outstanding superionic conductivity. *Chem. Mater.* **2015**, *27*, 5483–5486. [CrossRef]
29. Hwang, S.-J.; Bowman Jr, R.C.; Kim, C.; Zan, J.A.; Reiter, J.W. Solid State NMR Characterization of Complex Metal Hydrides systems for Hydrogen Storage Applications. *J. Anal. Sci. Technol.* **2011**, *2*, A159–A162. [CrossRef]
30. Heřmánek, S. B NMR spectra of boranes, main-group heteroboranes, and substituted derivatives: Factors influencing chemical shifts of skeletal atoms. *Chem. Rev.* **1992**, *92*, 325–362. [CrossRef]
31. Verdal, N.; Her, J.-H.; Stavila, V.; Soloninin, A.V.; Babanova, O.A.; Skripov, A.V.; Udovic, T.J.; Rush, J.J. Complex high-temperature phase transitions in $Li_2B_{12}H_{12}$ and $Na_2B_{12}H_{12}$. *J. Solid State Chem.* **2014**, *212*, 81–91. [CrossRef]
32. Remhof, A.; Yan, Y.; Rentsch, D.; Borgschulte, A.; Jensen, C.M.; Züttel, A. Solvent-free synthesis and stability of $MgB_{12}H_{12}$. *J. Mater. Chem. A* **2014**, *2*, 7244–7249. [CrossRef]
33. Nakamori, Y.; Miwa, K.; Ninomiya, A.; Li, H.; Ohba, N.; Towata, S.-I.; Züttel, A.; Orimo, S.-I. Correlation between thermodynamical stabilities of metal borohydrides and cation electronegativites: First-principles calculations and experiments. *Phys. Rev. B* **2006**, *74*. [CrossRef]
34. Guo, Y.; Jia, J.; Wang, X.-H.; Ren, Y.; Wu, H. Prediction of thermodynamically reversible hydrogen storage reactions in the KBH_4/M (M= Li, Na, Ca)$(BH_4)_n$ (n = 1, 2) system from first-principles calculation. *Chem. Phys.* **2013**, *418*, 22–27. [CrossRef]